RESIDUAL STRESSES AND FRACTURE TOUGHNESS OF AN $Al_2O_3/Al_2O_3 + ZrO_2$ LAYERED CERAMICS

T. Köves, J. Dusza, G. de Portu

Abstract

Different methods (the analytical model, finite element calculation, and experimental method) have been used for the residual stress evaluation in the individual layers of a layered Al_2O_3 / Al_2O_3 + ZrO_2 composite. The microstructure characteristics and indentation fracture toughness of the individual layers have been investigated. Influence of the residual stresses on the fracture toughness anisotropy and crack propagation in the individual layers have been studied. Based on the calculated residual stress level in the individual layers the apparent R-curve behaviour was calculated.

Keywords: layered ceramics, residual stresses, fracture, R-curve

INTRODUCTION

Structural ceramics have a number of excellent properties, however their wider application is still limited by their brittleness, low flaw tolerance and low reliability. Therefore the production of large load-bearing or rapidly rotating parts, which are subjected to high mechanical loads at high temperatures, is very difficult. Their low flaw tolerance – high brittleness – is strongly connected with the presence of ionic or covalent atomic bonds and with the limited number of independent slip systems which are cooperative when compared with the number of those which are necessary for plastic deformation commonly observed in metals and alloys [1,2].

Different approaches have been used during the last two decades with the aim to improve room temperature properties, reliability, life span, and high temperature properties of structural ceramics. One of the often used approaches – the laminar structure approach [3,4] – improves the structural reliability by designing novel laminar composites which promote crack deflection on interlayer boundaries and/or utilize compressive residual stresses generated during cooling down from the sintering temperature as a result of differences in thermal expansion coefficients between layers with different compositions.

Various techniques have been used during the last decade to produce laminar/layered composites: rolling, tape casting, slip casting, centrifugal casting, electrophoretic deposition or simple layering [5,6]. Clegg et al. [5] used surface treated carbon or silicon carbide sheets which are compacted in order to form the desired shape and pressurelessly sintered. The silicon carbide sheets are fabricated using α-SiC, β-SiC and boron mixed with an aqueous solution of polyvinyl alcohol and extruded, then pressed, and rolled to a thickness of approx. 200 μm. After this, the sheets are coated with a suspension of colloidal graphite, pressed together, and sintered.

Tape and slip casting is used for fabrication of different oxide based laminar/layered composites [6]. The slurry formation is optimized according to two criteria: by increasing the relative portion of dry matter and by increasing the elimination rate of

Tibor Köves, Ján Dusza, Institute of Materials Research, Košice, Slovak Academy of Sciences, Slovak Republic
Goffredo de Portu, Research Institute for Science and Technology for Ceramics (ISTEC), Faenza, Italy

organic components during heat-treatment. Slurries with different chemical composition are tape cast to laminates with a thickness from 100 to 200 μm.

Multi-layered composites are fabricated by periodic stacking of different layers. After removal of the organic additives the bulk material is pressed or cold isostatically pressed and then sintered or hot pressed. Similarly, multilayer composites are obtained by alternate drain casting of suspensions with different composition for fixed casting times. Multilayered composites with alternating layers of different oxide ceramics have been fabricated using a colloidal technique [7,8]. This involves sequential centrifugation of solutions containing suspended particles to form a green body. After drying the composite is sintered. Uniform layers with thickness in a range from 10 to 100 μm have been obtained using this technique.

The synthesis of laminar micro-composites is carried out by electrophoretic deposition. Using this method, layers with a minimal thickness of 2 μm were deposited sequentially on a graphite electrode, then dried and sintered [8].

Three- and multilayered silicon nitride based composites are prepared with layer thicknesses from 0.1 to 2 mm [9,10]. The individual layers (Si_3N_4 with sintering additives, with SiC or TiC) are pressed using a steel die, then cold isostatically pressed. The compacted layers are stacked with alternate sequences of different composition and pressurelessly sintered or hot pressed.

Layered ceramics can be divided into three main groups according to the mechanisms for increasing their mechanical properties: composites with constrained transformation zones [11,12], composites with tailored residual stresses [13-15], and composites with weak interfaces. In the layered composites of the fourth category different mechanical responses of the individual layers are combined in order to produce a composite with properties which, for some applications, are superior to those of the constituent ceramics [16-18].

In layered/laminar composites residual stresses can be developed during cooling down from the sintering temperature due to the different thermal coefficients of the layers. The sign and magnitude of these stresses can be tailored by composition of the individual layers but also by the thickness of layers [13-15].

The aim of the present contribution is to study and compare different methods for residual stress evaluation as well as to study the influence of residual stresses on the fracture toughness anisotropy in the individual layers and through the layers of an $Al_2O_3/Al_2O_3 + ZrO_2$ layered composite.

EXPERIMENTAL MATERIAL AND METHODS

The experimental material was prepared at the National Research Council, Institute of Science and Technology for Ceramics, Faenza, Italy. A laminar composite consisting of a regularly alternated stacking of layers made from Al_2O_3 and 60 vol% Al_2O_3 + 40 vol% ZrO_2 – containing 3 mol% of Y_2O_3 - (ZTA) was fabricated by tape casting, followed by manner moulding of different layers, binder burn-out, and sintering, Toschi [19]. In such a way composite plates (3 x 28 x 42 mm) formed of 9 layers were prepared. The specimens were cut in bars with dimensions of 3 x 4 x 42 mm and polished to 1 μm finish. Microstructure of the investigated material was studied after a thermal etching using scanning electron microscopy (SEM). Analytical method, finite element modelling, and experimental methods have been used to evaluate residual stresses in the individual layers. Equations (1,2) have been used for residual stress calculation by the analytical method [20,21]:

$$\sigma_A = -\frac{E_A E_B (n+1)(\alpha_B - \alpha_A)(T_1 - T_2)}{xnE_B(1-\nu_A) + E_A(n+1)(1-\nu_B)} \quad (1)$$

$$\sigma_B = \frac{xnE_A E_B (\alpha_B - \alpha_A)(T_1 - T_2)}{xnE_B(1-\nu_A) + E_A(n+1)(1-\nu_B)} \quad (2)$$

where: E – Young's modulus, n – number of the layers B, α – thermal expansion coefficient, T_1 – sintering temperature, T_2 – operating temperature (in this case room temperature), ν – Poisson's ratio.

The relation between indentation load, fracture toughness and the length of the indentation crack can be described by the equation:

$$K_{IC} = \chi \cdot \left(\frac{P}{c_0^{\frac{3}{2}}} \right) \quad (3)$$

where: K_{IC} – toughness of the stress-free material, χ – dimensionless constant, P – indentation load, c_0 – crack length.

The value of parameter $\chi \doteq 0.089$ was found by regression analysis from the values of P, c_0 and the fracture toughness for monolithic alumina K_{IC} = 3.61 MPa.m$^{1/2}$ measured by the Chevron notch technique [19].

In the event that residual stresses are present in the material, from the Eq. (3) becomes

$$K_{IC} = \left(\frac{P}{c_1^{\frac{3}{2}}} \right) + Y \cdot \sigma_{res} \cdot c_1^{\frac{1}{2}} \quad (4)$$

where: c_1 – crack length in the stressed material, Y = 1.29, σ_{res} – residual stress value.

The residual stresses can be calculated with Eq. (4).

The finite element method is used in a wide variety of engineering disciplines for solving different scientific problems. A number of authors used this method to model residual stresses in layered ceramic systems. The MSC Marc program system for finite element calculations has been used in this investigation.

From the results of FEM, the residual stresses from the center line, the middle of the surface, and at the corner of the specimens were used only (Fig.1). Knowing the overall dimensions as well as the material properties, a 3D solid model was constructed. The element size was ~ 0.14 mm x 0.14 mm, and it is width depended on the layer width. Each layer was divided into 10 element rows in the direction perpendicular to the layers' width. The element type was hex8. At first calculation, the Al_2O_3 layer width was 193 μm and the width of the Al_2O_3+ZrO_2 layer was 529 μm. When creating the model the symmetry of the specimen was considered. Symmetrical boundary conditions have been used, therefore it was enough to calculate with 1/8th part of the original specimen (Fig.1). The calculation method and the material model were linear.

Influence of the width ratio of layers on the magnitude and distribution of residual stresses has been calculated. The overall dimensions were the same as in the first

calculation, but the layer width ratios (Al_2O_3 : Al_2O_3+ZrO_2) were changed between 1 : 1 and 1 : 10 (Table 1). All other parameters (for example: Young's modulus, Poisson's ratio, moulding temperature) were not changed. The residual stresses were investigated in the center line, in the middle of the surface, and at the corner of the specimens.

The indentation fracture toughness was investigated using a Vickers hardness testing device at indentation loads of 50, 100, and 150 N. Fractographic analyses of the indented specimens were carried out using optical and scanning electron microscopy [22,23].

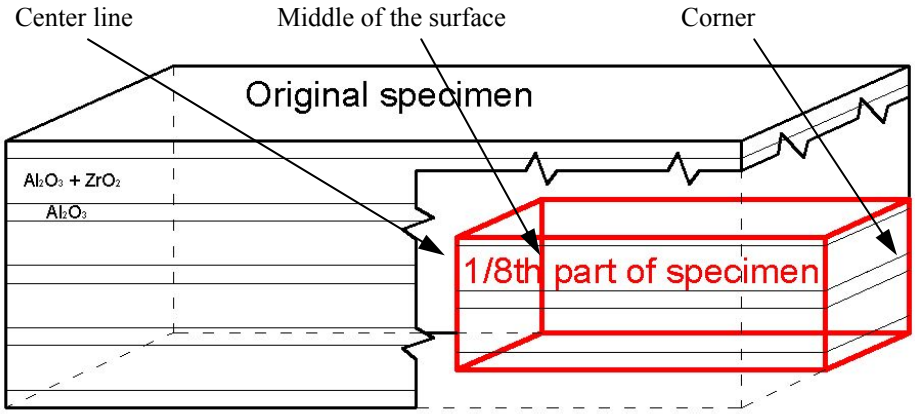

Fig.1. Symmetrical boundary conditions for Al_2O_3 – Al_2O_3+ZrO_2 composite.

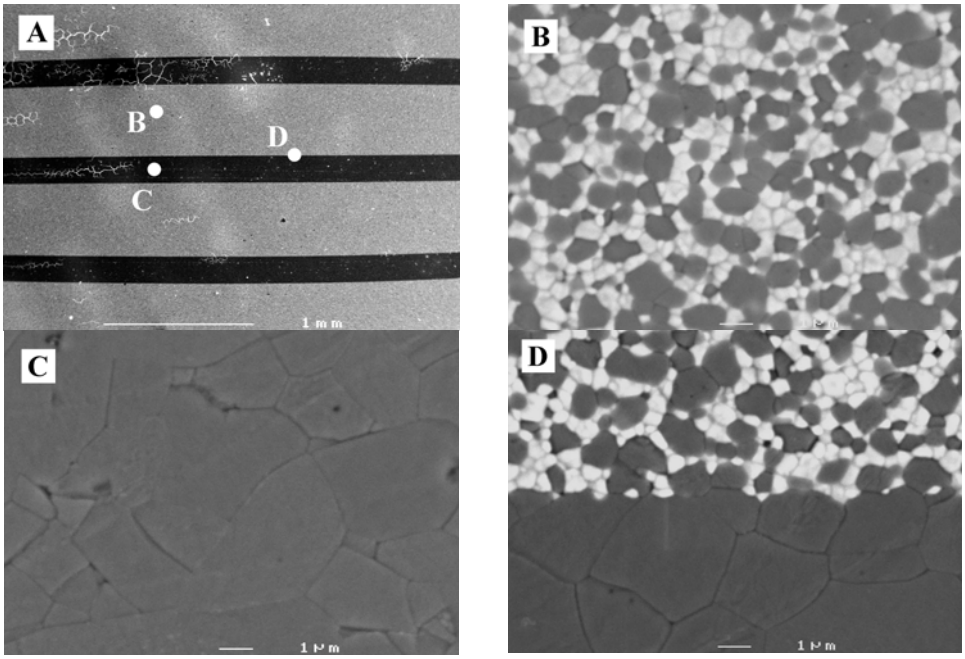

Fig.2. Macrostructure of the specimen (A) and microstructure of both layers (B, C) and their boundary (D).

RESULTS AND DISCUSSION

Characteristic micro- and macrostructure of the individual layers and boundaries are illustrated in Fig.2. The cross-section of the specimen with thinner Al_2O_3 layers (dark area) and thicker ZTA layers (bright area) is illustrated together with details of the individual layers (Fig.2b, c) and of the layer boundary (Fig.2d), respectively. The thickness of the Al_2O_3 layers was 193 ± 5 μm, while that of Al_2O_3 + ZrO_2 was 529 ± 15 μm. According to the results, the mean grain size of Al_2O_3 in the Al_2O_3 + ZrO_2 layer (0.69 ± 0.3 μm) is significantly lower when compared with the grain size in the pure Al_2O_3 layer (2 ± 1.1 μm) and the size distribution in the Al_2O_3 + ZrO_2 layer is narrower as well. The average grain size of the ZrO_2 in the Al_2O_3 + ZrO_2 layer is 0.27 ± 0.25 μm.

For the residual stress in the Al_2O_3 layer of the Al_2O_3/Al_2O_3 (60%) + ZrO_2 (40%) composite there is a value of $\sigma_{Al2O3} = \sigma_1 = -405$ MPa (compression), and in the Al_2O_3+ZrO_2 layer $\sigma_{Al2O3+ZrO2} = \sigma_2 = 148$ MPa (tension) was calculated using Eqs. (1,2).

Using FEM, the residual stress in the Al_2O_3 layer of the Al_2O_3/Al_2O_3 (60%) + ZrO_2 (40%) composite has a value of $\sigma_{Al2O3} = \sigma_1 = -405.5$ MPa (compression), and in the Al_2O_3 + ZrO_2 layer $\sigma_{Al2O3+ZrO2} = \sigma_2 = 216.6$ MPa (tension) was calculated.

Using Eq. (4), for the residual stress in the Al_2O_3 layer of the Al_2O_3/Al_2O_3 (60%) + ZrO_2 (40%) composite a value of $\sigma_{Al2O3} = -214.2$ MPa was obtained.

Comparing the residual compression stresses received from different methods it can be stated that the theoretically calculated stresses using the analytical model and FEM are in very good agreement and the experimentally measured values are lower in comparison with them.

The results are in a good agreement with the results of [24,25] and are probably caused by the residual stress relaxation on the free surface of the specimens where the experimental measurements have been realized.

Influence of the layer width ratios on the theoretically and FEM calculated residual stresses are illustrated in Tables 2 and 3.

Tab.1. Applied layers width ratios and layer widths.

Layer width ratio	Al_2O_3 layer width [μm]	Al_2O_3 + ZrO_2 layer width [μm]
1:1	342.33	342.33
1:2	237.00	474.00
1:3	181.24	543.71
1:4	146.71	586.86
1:5	123.24	616.20
1:6	106.24	637.45
1:7	93.36	653.55
1:8	83.27	666.16
1:9	75.15	676.32
1:10	68.47	684.67

Tab.2. Theoterically calculated maximum and minimum residual stresses in the case of different layers width ratios.

Stress type	Layer width ratio (Al_2O_3 : Al_2O_3 + ZrO_2)									
	1:1	1:2	1:3	1:4	1:5	1:6	1:7	1:8	1:9	1:10
Compression	-259.4	-362.1	-416.9	-451.1	-474.5	-491.5	-504.4	-514.6	-522.7	-529.4
Tension	259.4	181.0	139.0	112.8	94.9	81.9	72.1	64.3	58.1	52.9

Tab.3. FEM calculated maximum and minimum residual stresses in case of different layers width ratios (global min. and max. values).

Stress type	Layer width ratio (Al_2O_3 : $Al_2O_3 + ZrO_2$)									
	1:1	1:2	1:3	1:4	1:5	1:6	1:7	1:8	1:9	1:10
Compression	-260.4	-362.1	-417.2	-451.7	-475.2	-492.4	-505.3	-515.5	-523.7	-530.4
Tension	307.4	244.2	209.0	186.7	169.7	157.5	147.0	138.3	130.4	123.4

Comparing the results of Tables 2 and 3 it is possible to say that the compression residual stresses are in a very good agreement, but the residual tensile stresses are different and this difference is growing with increasing width ratio of the layers. This is probably caused by the error of the theoretical model.

The stress distribution through the layers of the composite is illustrated in Fig.3. It is visible that there are significant differences in the residual stress values in the centre, middle of the surface, and in the corner of the specimen. The highest residual stresses (both tensile and compressive) are in the volume of specimen, those on the surface are lower, and their stress distribution is different as well.

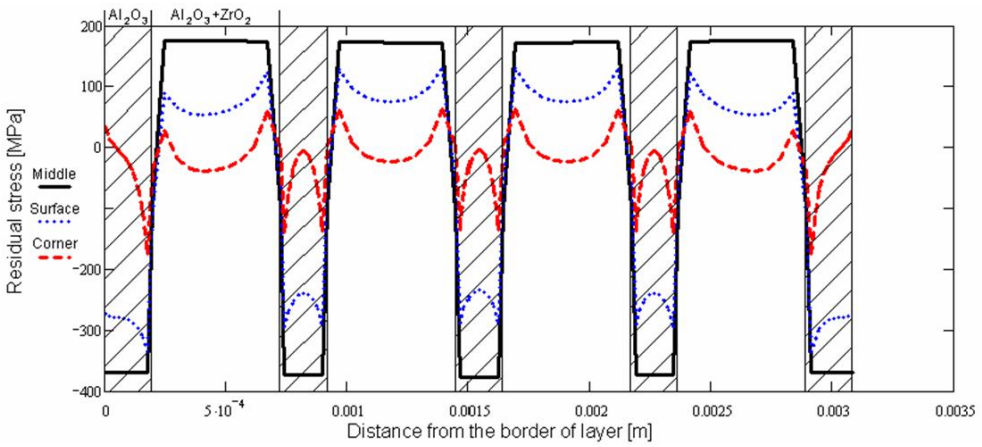

Fig.3. Stress distribution through the layers (FEM result).

The average Vickers hardness values and values of the indentation fracture toughness in directions parallel (II) and perpendicular (T) to the layers are illustrated in Tables 4 and 5.

The indentation fracture toughness test revealed the presence of toughness anisotropy. In the Al_2O_3 + ZrO_2 layers the anisotropy is less evident and the fracture toughness values are slightly lower in the direction perpendicular to the layers, in comparison to those measured parallel with the layers. In the Al_2O_3 layer the toughness anisotropy is more evident and the K_{IC} values are higher when measured perpendicularly to the layers in comparison with those measured parallel to the layers.

Tab.4. Macrohardness and indentation fracture toughness in directions parallel (II) and perpendicular (T) to the layers for Al_2O_3.

Layer	Al_2O_3		
Load [kg]	HV	K_{IC}II [MPa.m$^{1/2}$]	K_{IC}T [MPa.m$^{1/2}$]
5	1548 ± 70	1.39 ± 0.23	6.16 ± 0.59

Tab.5. Macrohardness and indentation fracture toughness in directions parallel (II) and perpendicular (T) to the layers for $Al_2O_3 + ZrO_2$.

Layer	$Al_2O_3 + ZrO_2$		
Load [kg]	HV	K_{IC}II [MPa.m$^{1/2}$]	K_{IC}T [MPa.m$^{1/2}$]
5	1337 ± 36	7.54 ± 0.74	5.14 ± 0.45
10	1353 ± 35	6.93 ± 0.46	4.35 ± 0.47
15	1386 ± 25	7.17 ± 1.03	3.42 ± 0.25

The measured indentation fracture toughness values are in a good agreement with the present residual stresses. Higher fracture toughness measured perpendicularly to the layer plane is due to the presence of compressive residual stresses in the Al_2O_3 layers. On the other hand, tensile residual stresses in the Al_2O_3+ZrO_2 layer results in a lower fracture toughness perpendicular to the layer plane.

Large differences were found when comparing the fracture toughness values measured in the Al_2O_3 inner layer (when the indentation direction was paralel to the layers plane), with those achieved by indentation tests on the outer Al_2O_3 layer (when the indentation direction was perpendicular to the layers plane). The fracture toughness of the outer layer measured at the load of 50 N was 5.54 MPa.m$^{1/2}$, which is lower than the value of 6.16 MPa.m$^{1/2}$ measured for the inner Al_2O_3 layer.

Based on the calculated residual stresses, the apperent R-curve of the layered composite can be calculated.

According to the Griffith failure criterion :

$$K = \sigma \cdot Y \cdot \sqrt{a} \geq K_{IC} \tag{5}$$

where: K – Stress intensity factor, σ – Characteristic stress,Y – Geometric function, a – Crack size, K_{IC} – Fracture toughness.

An external crack in the specimen is considered for calculation. The stress distribution before the crack tip in the not cracked part of the specimen in the hypothetical crack direction is σ(x). The stress intensity factor for this stress distribution is given by [26]:

$$K_{residual} = K_I = \int_0^a \sigma(x) \cdot h(x,a) \cdot dx \tag{6}$$

where: h(x,a) – weight function.

The integration has to be performed along the crack length from x=0 at the surface until x = a. The weight function h(x,a) depends on the geomery of the layer and on the crack length. For an edge crack in a bar shaped specimen, the weight function is given by [27]:

$$h(x,a) = \sqrt{\frac{2}{\pi \cdot a}} \cdot \frac{1}{\sqrt{1-\frac{x}{a}} \cdot \left(1-\frac{a}{W}\right)^{\frac{3}{2}}} \cdot \left[\left(1-\frac{a}{W}\right)^{\frac{3}{2}} + \sum A_{ij} \cdot \left(1-\frac{x}{a}\right)^{i+1} \cdot \left(\frac{a}{W}\right)^{j} \right] \tag{7}$$

where: W – width of the specimen.

Tab.6. Values of the coefficient A_{ij} for Eq. (7) [20].

	j=0	j=1	j=2	j=3	j=4
i=0	0.4980	2.4463	0.0700	1.3187	-3.067
i=1	0.54165	-5.0806	24.3447	-32.7208	18.1214
i=2	-0.19277	2.55863	-12.6415	19.763	-10.986

Each material, in this case each layer has its own fracture toughness value, which is $K_{intrinsic}$. The apparent R-curve is given by [28]:

$$K_R = K_{intrinsic} - K_{residual} \tag{8}$$

The apparent R-curve behaviour of the investigated material/specimen is illustrated in Fig.4. The layer thickness of the Al_2O_3 layer is 193 μm and the thickness of $Al_2O_3 + ZrO_2$ layer 529 μm.

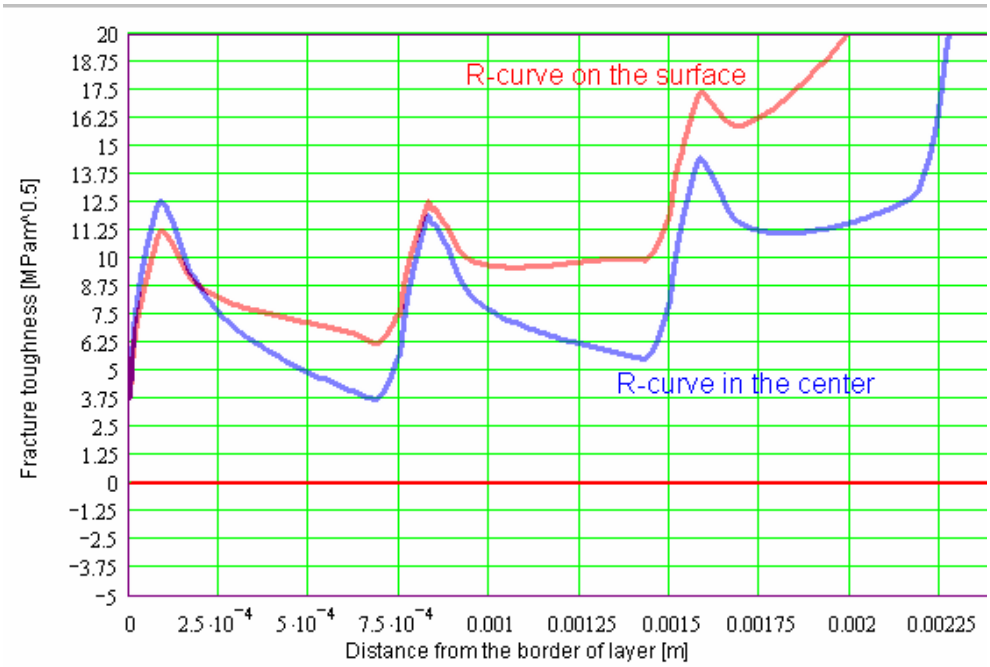

Fig.4. The apparent R-curve for $Al_2O_3/Al_2O_3 + ZrO_2$ layered composite with the thickness of Al_2O_3 layer 193 μm and $Al_2O_3 + ZrO_2$ layer 529 μm, respectively.

CONCLUSIONS

In this investigation different methods have been used and compared for the study of residual stresses in the individual layers of an Al_2O_3 / $Al_2O_3 + ZrO_2$ layered composite. Based on the calculated residual stress level in the individual layers the apparent R-curve behaviour was calculated. From the performed analyses of experimental data the following results were obtained:

- there is a very good agreement between the residual compression stresses calculated by analytical method and the finite element method (FEM);
- the residual compression stress calculated by indentation method is lower when compared with the analytical and FEM values;
- an evident fracture toughness anizotropy was found in individual layers due to the present residual stresses;
- the apparent R-curve of the layered composite was calculated based on the calculated stresses by the finite element method, which is strongly influenced by the residual stresses.

Acknowledgements

The work was partly supported by the European Community's Human Potential Programme under the contract HPRN-CT-2002-00203, [SICMAC], by NANOSMART, Centrum of Excellence of SAS, Slovak Grant Agency for Science via grant No. 2/4173/04, and by the Science and Technology Assistance Agency under the contract No. APVT – 51 – 049702.

Tibor Köves acknowledges the financial support provided through the European Community's Human Potential Programme under the contract HPRN-CT-2002-00203, [SICMAC].

REFERENCES

[1] Cook, RF., Pharr, GM. In: Materials Science and Technology, vol. 11, Mechanical properties of ceramics. Ed. M.V. Swain. Weinheim : VCH, 1994, p. 339
[2] Becher, PF. In: Materials Science and Technology, vol. 11, Mechanical properties of ceramics. Ed. M.V. Swain. Weinheim : VCH, 1994, p. 339
[3] Harmer, MP., Chan, HM., Miller, GA.: J. Am. Ceram. Soc., vol. 75, 1992, p. 1715
[4] Clegg, WJ., Kendall, K., McN. Alford, N., Button, TW., Birchall, JD.: Nature, vol. 347, 1990, p. 455
[5] Clegg, WJ.: Acta Metall. Mater., vol. 40, 1992, p. 3085
[6] Requena, J., Moreno, R., Moya, JS.: J. Am. Ceram. Soc., vol. 72, 1989, p. 1511
[7] Marshall, DB., Ratto, JJ., Lange, FF.: J. Am. Ceram. Soc., vol. 74, 1991, p. 2979
[8] Nicholson, PS., Sarkar, P., Huang, X.: J. Mater. Sci., vol. 28, 1993, p. 6274
[9] Hyuang, JL., Chang, YL., Lu, HH.: J. Mater. Res., vol. 12, 1997, p. 2337
[10] Šajgalík, P., Lences, Z., Dusza, J.: J. Mater. Sci., vol. 31, 1996, p. 4837
[11] Marshall, DB., Ratto, JJ., Lange, FF.: J. Am. Ceram. Soc., vol. 74, 1991, p. 2979
[12] Marshall, DB.: Ceram. Bull., vol. 71, 1992, p. 969
[13] Chartier, T., Merle, D., Besson, JL.: J. Eur. Ceram. Soc., vol. 15, 1995, p. 101
[14] Amateu, MF., Messing, GL. In: International Encyclopedia of Composites. Ed. S.M. Lee. Vol. 3. Weinheim : VCH Verlag, 1900, p. 11
[15] Virkar, AV., Huang, JL., Cutler, RA.: J. Am. Ceram. Soc., vol. 70, 1987, p. 164
[16] Russo, CJ., Harmer, MP., Chan, HM., Miller, GA.: J.Am.Ceram. Soc., vol. 75, 1992, p. 3396
[17] Liu, H., Lawn, BR., Hsu, SM.: J.Am. Ceram. Soc., vol. 79, 1996, p. 634
[18] Lawn, BR., Lee, SK., Lee, KS. In: The science of engineering ceramics II. Ed. K. Niihara et al. Aedermannsdorf : Trans Tech Publications, 1998, p. 3
[19] Toschi, F., Melandri, C., Pinasco, P., Roncari, E., Guicciardi, S., De Portu, G.: J. Am. Ceram. Soc., vol. 86, 2003, no. 9, p. 1547
[20] Ceniga, L.: J. Therm. Stresses, vol. 27, 2004, p. 425
[21] Ceniga, L.: J. Therm. Stresses, vol. 27, 2004, p. 471

[22] Danzer, R.: Key Eng. Mat., vol. 223, 2002, p. 1
[23] Dusza, J., Steen, M.: Int. Mat. Rev., vol. 44, 1999, p. 1656
[24] Anné, G.: Mat.Sci.Forum, vol. 492/493, 2005, p. 641
[26] Hvizdoš, P.: Key Eng. Materials, vol. 290, 2005, p. 332
[27] Fett, T., Munz, D.: J. Am. Ceram. Soc., vol. 75, 1992, no. 11, p. 3133
[28] Fett, T.: Stress Intensity Factors and Weight Functions for the Edge-Cracked Plate Calculated by the Boundary Collacation Method. KfK Rept. No. 4791, Karlsruhe : Kernforschungszentrum Karlsruhe, 1990
[29] Javier, P., Chalvet, F., Lube, T., De Portu, G.: Key Eng. Mat., vol. 290, 2005, p. 214